Chapter II
Preparation and characterization

INTRODUCTION

The usefulness of ferrites is determined by their physico-chemical properties which fall into two categories-intrinsic and structure sensitive. The method of preparation needs heat treatment for the formation of crystal structure of material. For the preparation of ferrites various methods are used. For preparing a good quality ferrite, the most basic requirements are compositional control to achieve right combination of Ms, Hc, and k. The grain growth, densification and microstructural features develop during sintering process.

In this chapter, along with other methods of preparation, most widely accepted ceramic method is discussed in Section A, while in Section B the x-ray studies and in Section C the IR studies are discussed.

SECTION - A

2.1 METHODS OF FERRITE PREPARATION

Ferrites are prepared for the use of magnetic devices, either in polycrystalline or single crystal form. Different technique have been developed for the preparation of ferrites. Basically there are four steps in preparation of ferrite material.

1) Preparation of material to form an intimate mixture in the desired composition
2) Presintering

3) Converting the presintered material into fine powder and pressing the powder into required shape

4) Final sintering to form the end product.

There are four general methods for preparation of ferrite compositions. They are as follows -

2.1.1 CERAMIC METHOD

This is one of the most extensively used method in the commercial production of ferrites. High purity oxides are mixed together with the proportions required for the product. They are mixed and wet milled with steel balls for a few hours. After milling the mixture is dried and passed through the fine mesh screen. The mixture is calcinated at low temperature and then powdered and dried. This powder is then pressed into required shape with the help of hydraulic press and finally sintered at high temperature. The purity of the oxides and particle size and shape are important for desired application (1). They must posses high reactivity so that on mixing and after calcination a homogeneous ferrite can be prepared.

2.1.2 DECOMPOSITION METHOD

In this method, in place of oxides, salts like carbonates, nitrates and oxalates are used. They are mixed in the required proportions and preheated,

usually in the air, to form the oxides by thermal decomposition. The oxides formed by this method have ability to undergo solid state reaction (2). The other details of this method are similar to the above method.

2.1.3 HYDROXIDE PRECIPITATION METHOD

Attempts have been made to precipitate simultaneously the required hydroxides to avoid lengthy milling process involved in dry mixing. The precipitate contains the required metals in correct proportion. The knowledge of the solubility products of substances is essential in order to determine the pH value for complete precipitation. Economus (3) established this method for the preparation of ferrites and Wof et.al (4) have employed this method for rare earth garnets respectively.

2.1.4 OXALATE PRECIPITATION METHOD

Precipitation of metallic oxalate is preferable for two reasons. The first reason is that, precipitation can be carried out using ammonium oxalates, which will not leave any residue after heating. Secondly, most of metal oxalate have very similar crystal structure so that precipitation tends to produce mixed crystals which contain the metallic cations in exactly the same proportions in which they were present in the solution. Hence the mixing in the correct ratios can be achieved on a molecular scale

(3). If the precipitation occurs at widely different rates mixed crystals do not form uniformly.

2.2 SINTERING

Sintering process is the most important process which controls the extrinsic properties of ferrites. There are two steps of sintering, one is presintering and other final sintering.

2.2.1 PRESINTERING

According to Swallow and Jordon (5) the purpose of presintering is to -

1) decompose carbonates and higher oxides which reduce with the evolution of gas in final sintering
2) assist in homogenizing the material
3) smooth variation in supplies of raw materials
4) reduce or control the shrinkage which occurs during the final sintering.

During presintering the raw materials partly reacts to form the final product and amount of the reaction depends on the reactivity of components and on the presintering temperature.

2.2.2 FINAL SINTERING

For a good quality ferrite the grain size should be uniform. The pores should be intergranular

and no discontinuous grain growth should occur. This can be achieved in the final sintering process. The sintering is done to increase the density. The control of grain size and pore distribution has been reviewed by many authors (6.8). The microstructure mainly depends on the reactivity of the starting materials and sintering temperature.

2.2.3 SOLID STATE REACTION

According to Wagner(9) the spinel phase $Mg^{2+}Fe_2^{3+}O_4$ is formed at the interface of MgO^{2+} and $Fe_2^{3+}O_3$. The reaction proceeds by the counter diffusion of the cations Mg and Fe in the ratio 3:2 through practically rigid lattice of oxygen anions (Fig 2.1 a). If we provide the interface with marker in the ratio 1:3 the marker should be undergo no shift during the reaction. The ratio for $MgAl_2O_4$ is found to be 1:3 where as it is 1:2.7 for $MoFe_2O_4$ (10).

According to the Wagner model, in case of $MgAl_2O_4$ formation. The Fe_2O_3 of $MgFe_2O_4$-Fe_2O_3 phase boundary dissolves into the spinel phase without any loss of oxygen i.e. iron remains in the trivalent state. The dissolution of Fe_2O_3 into spinel is accompanied by the loss of oxygen. Assuming counter diffusion model with Mg^{2+} and Fe^{2+} instead of Mg^{2+} and Fe^{3+} and with oxygen transport through the gas phase the volume ratio of $MgFe_2O_4$ phase formed on both

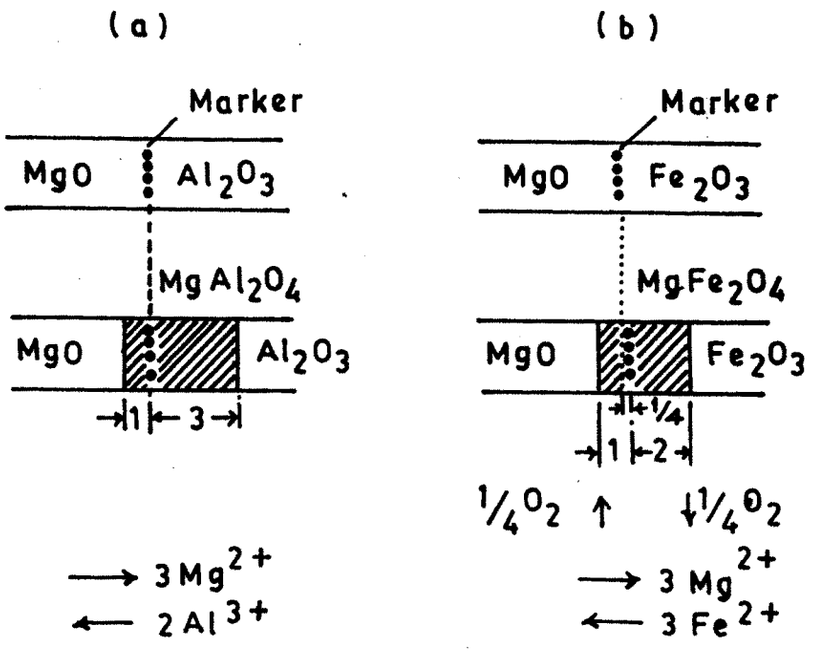

a) Counter diffusion of Mg^{2+} and Al^{3+} cations, no anion diffusion (Wagner mechanism).

b) Counter diffusion of Mg^{2+} and Fe^{2+} cations, no O^{2-} anion diffusion but reduction and oxidation of Fe ions at the respective phase boundaries which is equivalent to an oxygen transport through the gas phase.

Fig. 2·A·2 — MECHANISMS OF THE FORMATION OF a) $MgAl_2O_4$ AND b) $MgFe_2O_4$.

side of markers should be 1:2 and there should be smaller displacement of the markers. The effect is also called as Kirkendall effect (fig2.1b). This mechanism has the important consequence that the reaction becomes dependent on oxygen partial pressure. The reaction rate will increase by reducing conditions because large concentration gradient are set-up over the reaction layer and more Fe_2O_3 can dissolve into the spinel phase (11). It is proved earlier (12) that the formation of $MgFe_2O_4$ takes place due to Kirkendall effect. It is also reported that the similar phenomenon occurs during the formation of $NiFe_2O_4$ (13). The completion of solid state reaction can be confirmed by x-ray diffraction technique.

2.2.4 HOT PRESSING

The process of hot pressing has been increasingly used on an experimental scale during the last few years. Ferrites have been fabricated to very high density by hot pressing at low temperature. In this process, simultaneous application of temperature and pressure takes place (14). The powder is enclosed in a flexible container of rubber or plastic which may be evacuated and is compacted by immersing the container in an oil bath to which the pressure is applied. The effect is to give much more uniformity and high density than the conventional methods. It

also encourages continuous grain growth and favours to obtain low porosity and grain size. It seems apparent that pressure should lead to a high degree of compaction and enhance contact between grains during sintering. At 1000°C ferrites have sufficient plasticity to flow to a considerable extent at high pressures. It is favourable to produce high density compacts in which the original grain size is maintained.

2.3 ACTUAL METHOD FOR PREPARATION OF FERRITE SAMPLE

The ferrites samples with general formula $Ni_xFe_{3-x}O_4$ where x = 0.2, 0.4, 0.6, 0.8 and 1.0 were prepared by the standard ceramic method using pure nickel and iron oxide powders, the details of which are given below. A flow chart of preparation of ferrites is shown in Fig 2.2.

The high purity oxides of nickel and iron were weighed on the microbalance having least count of 0.001 gm and were mixed thoroughly in an agate mortar with acetone carefully without any loss of powder. The mixtures of powders were transferred in crucibles and presintered at 900 °C for 10 hours in air in a globar furnace. The furnace was cooled slowly. The temperature was measured by cromel-alumel thermocouple. The presintered powder was milled in a agate mortar

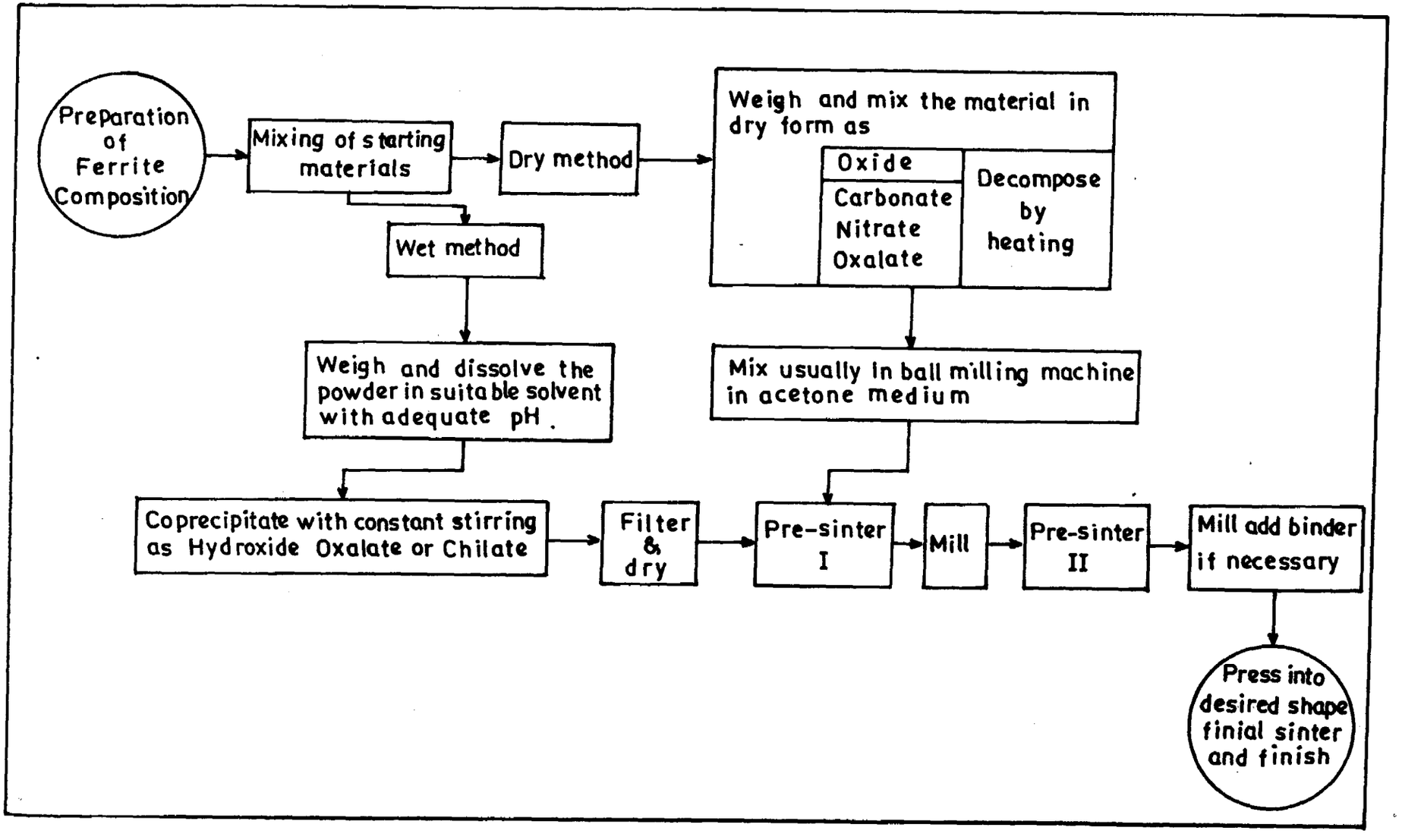

Fig. 2·A·1 – FLOW CHART OF STAGES INVOLVED IN PREPARATION OF FERRITES BY CERAMIC METHOD IN LAB.

with acetone for two hours and finally the powder was collected in a clean glass tube.

2.3.1 PELLET FORMATION

The dry powder was transferred into a die of 1 cm diameter and pressed in a hydraulic press with the pressure of about 6 to 8 tonnes per sq inch for about 3 to 5 minutes. After removing the load, pellets were taken out from the die. Five pellets of each composition were prepared by the same technique.

2.3.2 FINAL SINTERING

The pellets were placed in a crucible and kept in a globar furnace at a temperature of 1200 °C for 30 hours in air medium for the final sintering.

Three pellets of each composition were quenched in air, cold water, and magnetic field respectively. The applied field was about 4600 Gauss. The remaining pellets were slow cooled from 1200°C to room temperature.

SECTION - B

X-RAY DIFFRACTION STUDIES

2.4 INTRODUCTION AND PRINCIPLES OF X-RAY DIFFRACTION

X-ray diffraction technique is a well established tool to study the crystal structure of materials. The spinel structure of $MgAl_2O_4$ was first confirmed by Bragg (15) using x-ray diffraction

technique. The characterization of ferrites can be done by using x-ray diffraction. Electron and neutron diffraction are also employed in determining the crystal structure of ferrites. The neutron diffraction study of ferrites is carried out by the numbers of workers(16-18). In the present study X-ray diffraction is used to -

1) confirm the completion of solid state reaction
2) observe the impurity phases
3) determine the lattice constants, interplaner distances, octahedral and tetrahedral site radii and bond lengths etc.

According to Bragg's law, x-rays get diffracted from the planes (h k l) when the equation

$$2d_{hkl} \sin \theta = n \quad \ldots\ldots\ldots \quad 2.1$$

where d_{hkl} is the interplaner spacing of crystal planes of miller indices (h.k.l), θ is glancing angle, is wavelength of x-ray radiation and n is order of diffraction, is satisfied. In most cases, the first order diffraction where n = 1 is used and Bragg's law takes a form

$$= 2d_{hkl} \ \text{Sin}\ \theta \qquad \ldots\ldots\ 2.2$$

It can be shown that for the cubic crystal that

$$d_{hkl} = \frac{a}{\sqrt{h^2 + k^2 + l^2}} \qquad \ldots\ldots\ 2.3$$

where a is the lattice constant.

From equation 2.2 and 2.3 we get for lattice parameter

$$a = \frac{\lambda}{2 \sin \theta} [\sqrt{h^2 + k^2 + l^2}] \quad \ldots \quad 2.4$$

2.5 EXPERIMENTAL METHODS OF X-RAY DIFFRACTION

The methods of x-ray diffraction are as follows -

2.5.1 LAUE METHOD

In this method the crystal is kept stationary in a beam of continuous x-rays. The crystal selects a suitable wavelength (λ) and diffraction occurs from a plane with incident glancing angle (θ).

2.5.2 ROTATING CRYSTAL METHOD

In this method a crystal is rotated about a fixed axis in a beam of x-rays having fixed wavelength. For a particular value of θ Bragg's law is satisfied and diffraction occurs.

2.5.3 POWDER METHOD

This is the most widely used method of x-ray diffraction of polycrystalline samples. In this method the fine grained powder is filled in a capillary tube. The diffraction occurs simultaneously from the individual crystallites that happen to be oriented with planes having the same angle of incidence θ. In this method the wavelength is fixed and crystal is rotated. Recently, the counter diffractometers have been developed and are commercially available to record the diffractograms. In the counter diffractometer, the

sample is placed at the center, so that x-rays fall on the plane surface of the sample. About the same axis, rotates an arm carrying a Geiger counter which records the diffracted x-rays. When the sample is rotated by an angle Ø, the counter is turned through 2Ø. After complete scanning the XRD machine gives a record showing the variation of intensities of diffracted x-rays with angle Ø. This method was first developed by Debye and Scherrer (19) and independently by Hull (20).

2.6 EXPERIMENTAL TECHNIQUES

The x-ray diffraction patterns of the samples in the present case were recorded with the help of computerized XRD unit (Philips Model- APD 1710) with Cuk radiation (λ = 1.5418 A°) at USIC, Shivaji University, Kolhapur. The x ray diffraction patterns were taken with 2Ø values ranging between 20° to 80°.

2.7 RESULTS AND DISCUSSION

The X-ray diffraction patterns of $Ni_xFe_{3-x}O_4$ ferrites are shown in Figs. 2.3 to 2.5.

The standard spinel lattice of ferrite possesses the lattice parameter between a = 8.33 A° to 8.39 A°. The planes that diffract x-rays in cubic spinel systems are (111), (220), (311), (222), (400), (333) (440) etc. For all spinel ferrites (311) planes

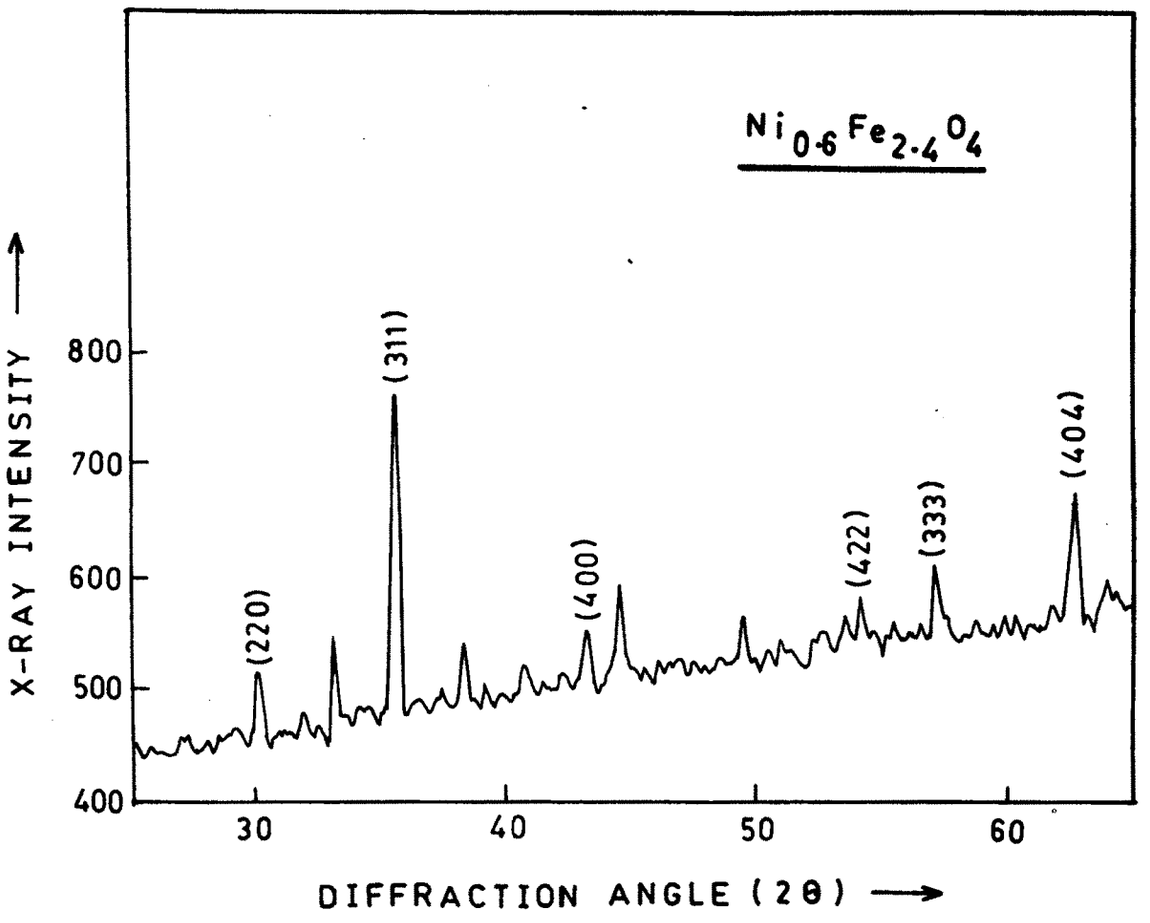

Fig. 2·3 —X-RAY DIFFRACTION PATTERN OF $Ni_{0.6}Fe_{2.4}O_4$.

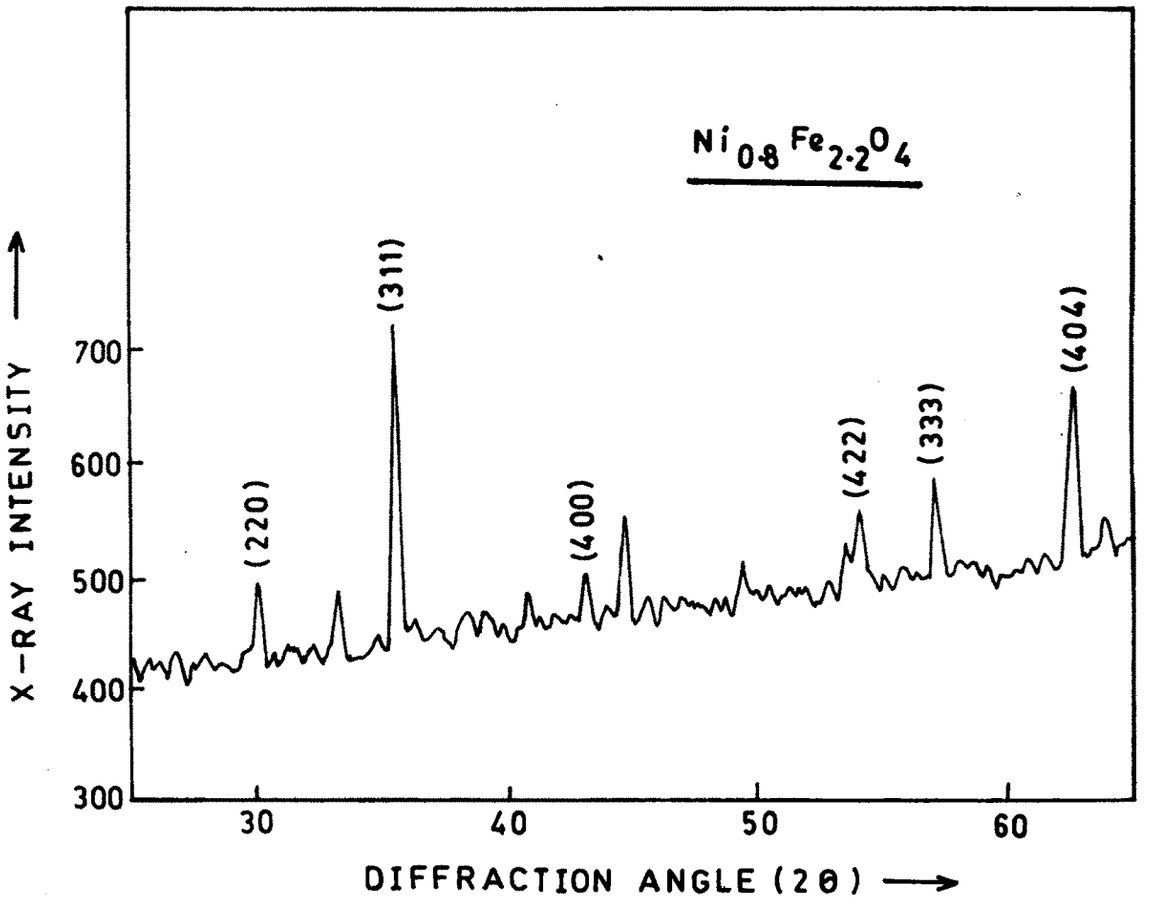

Fig. 2·4 – X–RAY DIFFRACTION PATTERN OF $Ni_{0·8}Fe_{2·2}O_4$.

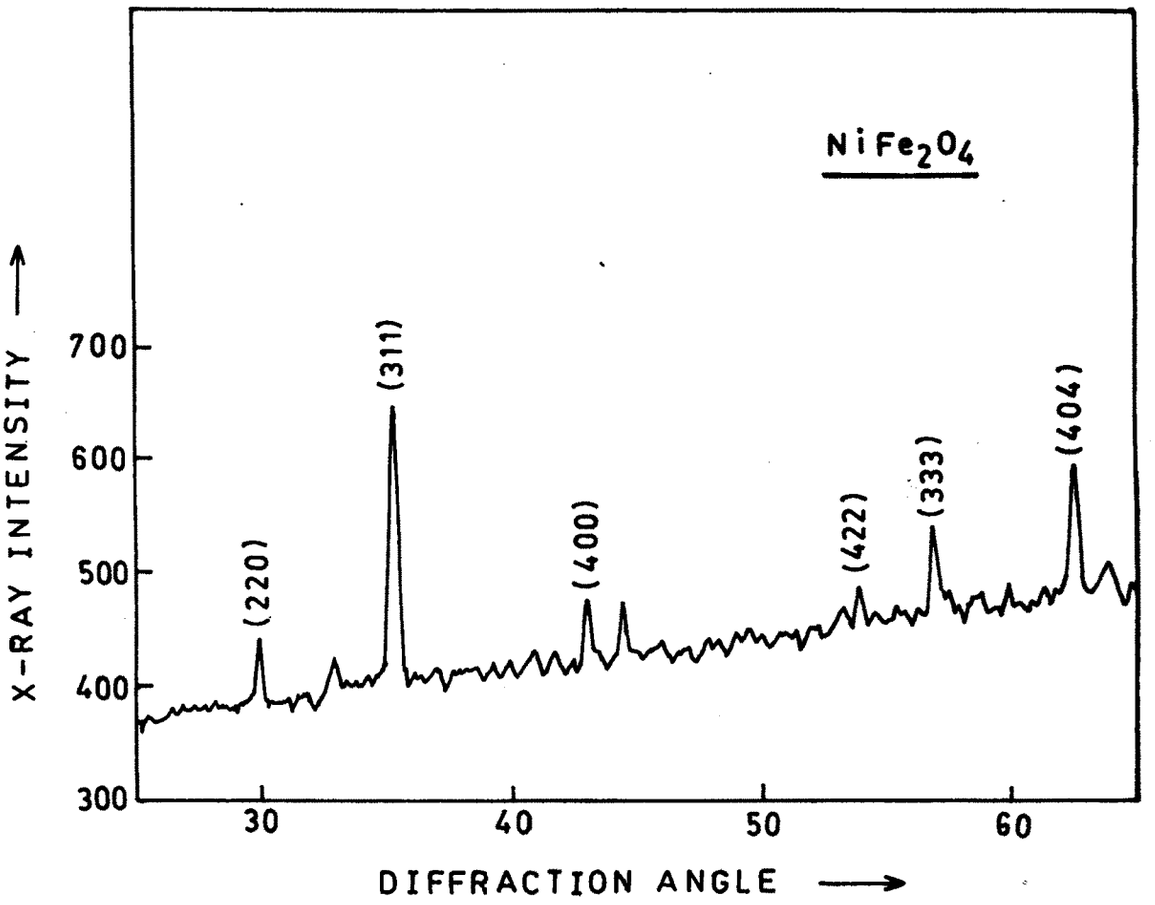

Fig. 2.5 – X–RAY DIFFRACTION PATTERN OF $NiFe_2O_4$.

is the most intense one. The lattice parameter a is calculated from observed d values of (311) planes.

The interplaner distance (d) for each diffraction angle was calculated by the relation (2.3). The observed and calculated d values are tabulated in Tables 2.1 to 2.5. It can be seen that the observed and calculated d values are in good agreement for all indexed planes. From diffraction patterns, it is observed that there are no extra lines, the fact which can be regarded as the confirmation of single phase ferrite formation.

The lattice parameters of each sample are given along with tables of d values. They were calculated by using relation (2.4). The values of lattice parameters come out to be 8.39 A in the present case, which is slightly larger than the values reported earlier. For Nickel ferrite the reported lattice parameters are 8.335 (21) and 8.339 (22,23) which are lower than the lattice constant calculated by us. This is attributed to the cation distribution.

The value of lattice parameter in the system $Ni_xFe_{3-x}O_4$ do not represent the absolute value. As the larger Ni^{2+} ions replace the smaller ferric ions on tetrahedral sites, these sites expand thereby initially enlarging the Medulung constant. The structure therefore begins the transformation to the more stable, normal structure. The removal of Ni^{2+} ions and

Table 2.1

X-ray diffraction data of $Ni_{0.2}Fe_{2.8}O_4$ ferrite
Wavelength - 1.5418 A°
lattice parameter a - 8.33 A°
Structure - Cubic

Sr. No.	2θ, deg	d_{calc}, A°	d_{obs}, A°	(hkl)
1	35.62	2.5176	2.5181	311
2	54.11	1.7044	1.6934	422
3	63.00	1.4760	1.4755	404

Table 2.2

X-ray diffraction data of $Ni_{0.4}Fe_{2.6}O_4$ ferrite
Wavelength - 1.5418 A°
lattice parameter a - 8.37 A°
Structure - Cubic

Sr. No.	2θ, deg	d_{calc}, A°	d_{obs}, A°	(hkl)
1	30.03	2.9663	2.9733	220
2	35.44	2.5206	2.5308	311
3	43.14	2.0975	2.0953	400
4	53.94	1.7126	1.6985	422
5	57.22	1.6146	1.6087	333
6	62.45	1.4831	1.4859	404

Table 2.3

X-ray diffraction data of $Ni_{0.4}Fe_{2.4}O_4$ ferrite
Wavelength - 1.5418 A°
lattice parameter a - 8.36 A°
Structure - Cubic

Sr. No.	2θ, deg	d_{calc}, A°	d_{obs}, A°	(hkl)
1	30.11	2.9557	2.9656	220
2	35.55	2.5206	2.5229	311
3	43.16	2.0900	2.0943	400
4	53.92	1.7064	1.7002	422
5	57.04	1.6088	1.6132	333
6	62.685	1.4778	1.4809	404

Table 2.4

X-ray diffraction data of $Ni_{0.8}Fe_{2.2}O_4$ ferrite
Wavelength - 1.5418 A°
lattice parameter a - 8.39 A°
Structure - Cubic

Sr. No.	2θ, deg	d_{calc}, A°	d_{obs}, A°	(hkl)
1	29.94	2.9733	2.9720	220
2	35.35	2.5357	2.5367	311
3	42.95	2.1025	2.1039	400
4	53.92	1.7166	1.6989	422
5	56.93	1.6185	1.6162	333
6	62.53	1.4866	1.4841	404

Table 2.5

X-ray diffraction data of $NiFe_2O_4$ ferrite
Wavelength - 1.5418 A°
lattice parameter a - 8.39 A°
Structure - Cubic

Sr. No.	2θ, deg	d_{calc}, A°	d_{obs}, A°	(hkl)
1	29.97	2.9733	2.9786	220
2	35.35	2.5357	2.5371	311
3	43.035	2.1025	2.1001	400
4	53.90	1.7166	1.6995	422
5	57.02	1.6185	1.6137	333
6	62.57	1.4866	1.4833	404

replacement of Ni^{3+} ion on octahedral sites relieves some of distortion on B site and allows the Ni^{3+} ions with their preference for B site, to replace once again Fe^{3+} ions on octahedral sites. The increase in lattice parameter also aids this process by decreasing u (21).

Using the value of u = 0.381 A of Nickel ferrite (2), the values of bond lengths (R_A and R_B) and site radii (r_A and r_B) were calculated using the relations

$$R_A = a\sqrt{3}\ (\delta + 1/8)$$

and

$$R_B = a\sqrt{1/16 - \delta/2 + 3\delta^2} \qquad \ldots \quad 2.5$$

$$r_A = (u - 1/4)\ a\sqrt{3} - Ro$$

and

$$r_B = (5/8 - u)\ a - Ro \qquad \ldots \quad 2.6$$

where R_A = Distance of cations from oxygen

R_B = Distance of anions from oxygen in B site

R_o = Radius of oxygen ion = 1.35A

r_A = Tetrahedral site radius

r_B = Octahedral site radius

δ = Deviation from oxygen parameter (u)

= u - Uideal [Uideal = 0.375 A)

The values of bond lengths (R_A and R_B) and site radii (r_A and r_B) are presented in Table 2.6. The bond length R_B is always greater than R_A. There is no remarkeable change in the bond length and site radii of the samples.

Table - 2.6

Data on bond lengths (R_A, R_B) and site radii (r_A, r_B) for $Ni_xFe_{3-x}O_4$ ferrites

x	R_A, A°	R_B, A°	r_A, A°	r_B, A°
0.2	1.8900	2.0333	0.54	0.68
0.4	1.9013	2.0455	0.55	0.69
0.6	1.8968	2.0406	0.54	0.68
0.8	1.9036	2.0482	0.55	0.69
1.0	1.9036	2.0482	0.55	0.69

Table 2.7

X-ray density, actual density and porosity data for $Ni_xFe_{3-x}O_4$ ferrites

x	d_{x-ray}(dx) gm/cc	d_{actual}(da) gm/cc	porosity, (P) %
0.2	5.3340	4.3836	21
0.4	5.2519	4.1171	27
0.6	5.3027	4.3122	18
0.8	5.2588	4.2834	18
1.0	5.2719	4.1258	21

The x-ray density (dx) and actual density (da) and porosity (P) of ferrite samples was calculated from the relations

$$dx = \frac{8M}{Na^3} \quad \ldots\ldots \quad 2.7$$

$$da = \frac{m}{\pi r^2 * t} \quad \ldots\ldots \quad 2.8$$

and $P(\%) = ((dx - da)/dx) * 100$ 2.9

where M = Molecular weight of sample

N = Avagadro's Number

a = Lattice parameter

m = mass of pellet

r = Radius of pellet

t = Thickness of pellet

Data on x-ray density, actual density and porosity is given in Table 2.7. The samples are about 20% porous.

SECTION - C

INFRA-RED STUDIES

2.8 INTRODUCTION

Electromagnetic radiations with wavelength 1 μ to 1 mm are known as infrared radiations. I.R spectroscopy in ferrites can be used to

1) detect the presence of absorption bands in ferrites

2) study of cation distribution.

3) study of deformation of cubic spinel structure

4) determine co-ordination of cations in spinel structure

Waldron (24) has studied IR spectra of some simple ferrites and has given the analysis in the region of 200 cm $^{-1}$ to 1000 cm^{-1}. He assigns the high frequency band (ν_1) at 600 cm^{-1} to tetrahedral complexes and low frequency band (ν_2) at 400 cm^{-1} to octahedral complexes.

Hafner (25), Tarte (26) and others (27,28) applied IR spectroscopy to study the absorption bands in many normal as well as inverse spinel ferrites.

In ferrites, two types of spectra are observed

1) Electronic spectra due to electronic transitions.

2) Vibrational spectra due to cation vibrations.

For the analysis of such spectra, it is necessary to consider a vibrational problem, which is most conveniently treated by classifying the crystals according to the continuity of bonding as (I) continuously bonded, (II) discontinuously bonded and (III) intermediates.

In the continuously- bonded crystals the atoms are bonded to all the nearest neighbours by the equivalent forces (ionic, covalent or van der walls) and frequency distribution of the vibration is given by Debye or Bornvan Karman treatment of classical mechanical problem and includes simple ionic crystals.

In the discontinuously bonded crystals, sets of atoms are tightly bonded by (intermolecular) chemical valance forces and seperated from adjacent sets by weak van der waal forces, examples - solid polyatomic gases, most organic compounds, non metallic compounds.

In third class, the intermolecular forces are somewhat greater than those in molecular cases and the branches may overlap and the vibrational problem may occasionally be treated as a perturbation of class-2 cases. Examples of this groups includes ionic crystals containing polyatomic ions, hydrogen-bonded crystals and strongly dipolar crystals.

2.9 EXPERIMENTAL TECHNIQUES

The IR spectra of all ferrite sample were recorded on Perkin Eimer 783 IR spectrometer. The pellets used for recording spectra were prepared by mixing small amount of ferrite powder in KBR. The IR spectra in the frequency range 200 - 800 cm^{-1} were recorded at room temperature. This facility is made available by USIC, Shivaji University, Kolhapur.

2.10 RESULTS AND DISCUSSION

The IR spectra of present samples are shown in Figs. 2.6 to 2.7. The spectra of all ferrite sample are used to locate the band positions which are

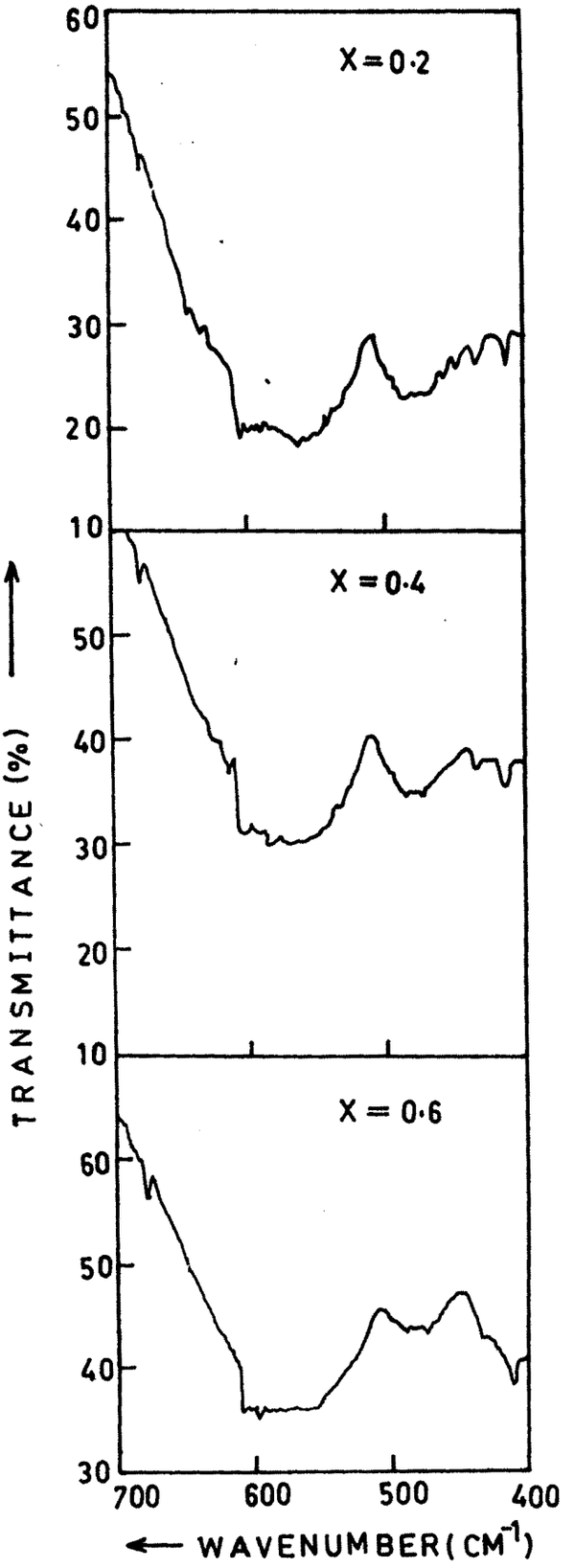

Fig. 2.6 – INFRARED SPECTRA FOR $Ni_x Fe_{3-x} O_4$ FERRITES.

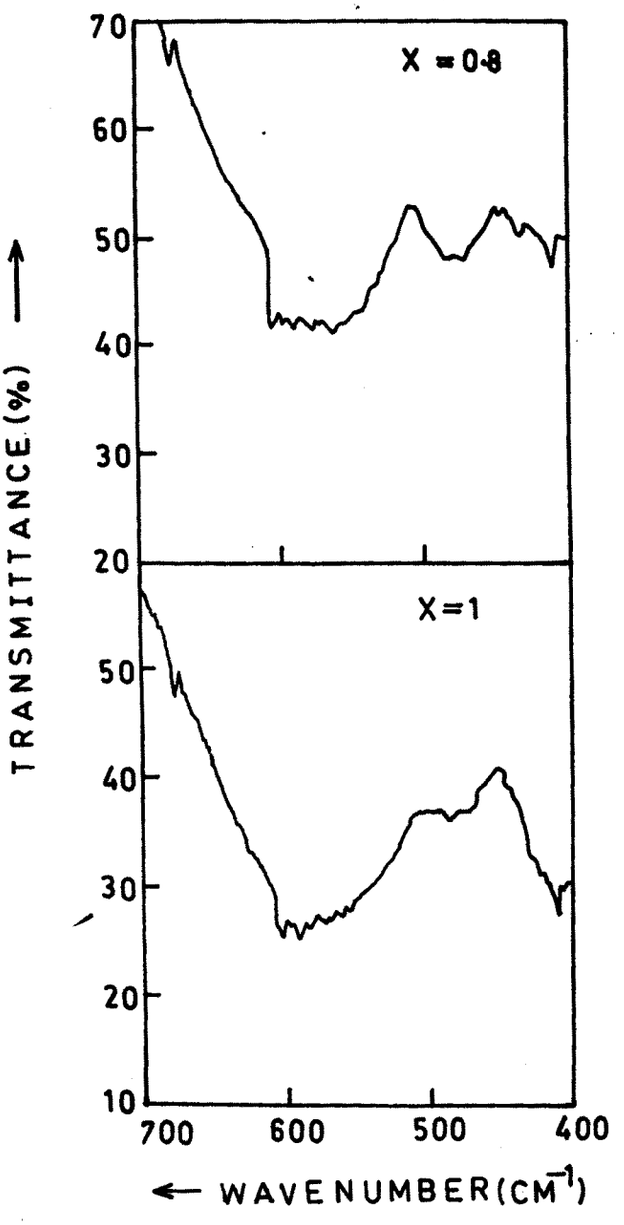

Fig. 2.7 – INFRARED SPECTRA FOR $Ni_x Fe_{3-x} O_4$ FERRITES.

noted in Table 2.8. It has been pointed out that vibrational frequencies depends on the mass of cations, bonding force, distance and unit cell dimensions (29). Brabers (30) has classified the lattice vibration of cubic spinel. According to his classification there are four IR active modes which are triply degenerate for the normal spinel. For inverse spinel and partly inverse spinels triply degenerate vibrations may split-up into three vibrations. If the splitting is not too large and there is certain statistical distribution of various cations over the tetrahedral and octahedral sites one cannot observe the splitting but only broadening of the absorption band. The broadening of spectral lines in the present spectra may be due to this reason. The Ni ferrite is inverse spinel therefore the statistical distribution of Fe is on both sites.

Generally, there are four absorption bands observed in ferrites. The absorption band ν_1 corresponds to streching of tetrahedral metal and oxygen band and $\nu 2$ is caused by oxygen vibrations in the direction perpendicular to tetrahedral ions, oxygen axis and other two absorption band ν_3 and ν_4 are associated with vibrations of metal ions in the isotropic force fields of their octahedral environment. They are located in the far infra-red region. Waldron (24) has studied IR spectra of number of ferrites and

Table 2.8

Lattice vibration frequencies for $Ni_xFe_{3-x}C_4$ ferrites

x	ν_1, cm^{-1}	ν_2, cm^{-1}
0.2	570	480
0.4	570	480
0.6	570	480
0.8	570	480
1.0	590	480

he has observed two broad bands for most of them. He attributed the band ν_1 (around 600 cm^{-1}) to tetrahedral complexes and ν_2 (around 400 cm^{-1}) to octahedral complexes and expected that ν_1 is greater than ν_2. Many other workers (31,26,29,32) have observed the IR spectra in ferrites and they were same as those of Waldron.

In present system higher frequency band is observed in the region 570 cm^{-1} - 590 cm^{-1} while lower frequency band is observed in the region at 480 cm^{-1}. This difference in the band position is expected because of difference in Fe^{3+}--O^{2-}-- distance for octahedral and tetrahedral complexes. The method for preparation, grain size and porosity can influence the location of band position. IR spectra can also be used to get the information about the valencies of cations in the spinel.

REFERENCES

1. Magee J. H., Morton V., Fisher R.D., and Loew I.J.
Ferrites Proc. Int. Conf., Japan (1970) 217

2. Standley K.J.
"Oxide Magnetic Materials",
Oxford Univ. Press, London ,(1962) 64

3. Economus G.
J. Amer. Ceram. Soc. 38 (1955) 241

4. Wolf W. P. & Rodrigue G.P.
J. Appl. Phys. 29 (1958) 105

5. Swallow D., Rodrigue G.P.,
J. Appl. Phys., 29 (1958) 105

6. Chol G., Damay F., Auradon J.P. and Strivens M.A.
Electrical Communications, 43 (1968) 263

7. Broese Van Groenou A.
Mat. Sci. Engng. 3 (1968) 317

8. Stuijts A.L.
Ferrites Proc. Int. Conf. ,Japan 108 (1970)

9. Wagner C.
Z. Phy. Chem. B-34 (1936) 309

10. Carter R.E.
J. Am. Ceram. Soc. , 44 (1961) 611

11. Reignen P.
"Science of Ceramic"
Stewart (ed.) Vol-3 Academic, N.Y. 1967

12. Kooy C.
"Material Transport in solid state Reaction"
Fifth Int. Symp. Reactivity Solids, Munich (1964)
p-21-28, Elsevier Amssterdam 1965

13. Elwell D., Parker R. and Tinsley C.Y.
Solid state communication, 4 (1966) 69

14. Murray P., Livey D. T. & Williams J.
"Ceramic Fabrication Processes"
W. D. Kingley (Edi),
Wiley, New York (1958) 147

15. Bragg W.L.
Nature (London) 95 (1915) 561

16. Shull C.G., Wollan E.O. & Koehlar W.C.
Phys. Rev. 84 (1952) 912

17. Hastings J.M. & Corliss L.M.
Rev. Mod. Phys. 25 (1953) 114

18. Prince E. & Treuting R. G.
Acta. Cryst. 9 (1956) 1025

19. Debye P. and Scherrer P.
Physic 17 (1916) 277 and 18 (1977) 219

20. Hull A.N.
Phy. Rev. 9 (1916) 564 and 10 (1917) 661

21. Wilson D.F. and Douglas D.L.
Material Science Monograph
15., Transport in Non-Stoichiometric Compounds
Proc. of First Int. Conf. Aug 27-30 (1980)

22. Kachi S.,Momiyama k., Shimizu S.
J. Phys. Soc. Japan, 18 (1963) 106

23. Takai T., Chiba S.
J. Phys. Soc. Japan, 21 (1966) 1255

24. Waldron R.D.
Phys. Rev. 99 (1955) 1727

25. Hafner S.T.
Z. Krist, 115 (1961) 331

26. Tarte P.
Spectrochim. Acta. 19 (1963) 49

27. Preudhomme J.
Spetrochim. Acta. 26-A (1970) 985

28. White R.B. and De Angelish B.A.
Spetrochim. Acta. 23-A (1963) 985

29. Murthy V.R.K., Chitrasankar S.,
Reddy K.V., Sobhanadri J.
Indian J. of Pure and applied Phys., 36 (1978) 79

30. Brabers V.A.M.
Physica Status Solidi (a) 33 (1969) 563

31. Pakhomova N.L. and Christopher V.
Phys. Stat. Solidi, (a) 105 (1987) 543

32. Reddy P. V. & Salagram M.
Physica Status Solidi (a) 100 (1987) 639